

A point-by-point reply to the comments

Reviewer 1#

5 I suggest the authors check the data again. Because all the discussions are based on the good quality data.

The explanation of the data inconsistency between figure 1 and previously published paper are still confusing.

10 The explanation indicated that the fitted data (background or polluted cases) have higher AR than the observed data (all averaged together). Does that suggest you need to check your fitting criteria/methods?

In addition, if there is calibration and correction method applied to the raw data. It will affect both observed data and fitted data. Why only observed data will have a slight lower MAF?

15 Re: Thanks for the suggestion. We do check the data carefully again. We are confident in the data quality. The reviewer is right, and if the correction is applied to the raw data, both the observed and fitted data will be affected. Thus, we also got a slight lower MAF for the fitted data (not shown in Figure 1). In the previously published paper, we didn't ignore and process some data points when the MAF value >1 , which resulted in larger mean MAF. But in this paper, the data points with MAF > 1.0 were forced to 1 when $D_p > 300$ nm, which we thought could be activated completely at even lower supersaturations but the MAF would never be >1.0 . This has been stated in the revised paper (please see Page 11, lines 199-204).

Reviewer 2#

25 P16147 L10 These "relative deviations" are because of particle loss in the nafion dryer? Also, it is not clear what the "kinetic limitations" are.

30 Re: the relative deviations are due to the influence of dehydration-related particle mobility changes inside DMA. According to Mikhailov et al., 2009, void fractions as well as residual water in dried aerosol particles that are not water-free (due to kinetic limitations of drying or stable hydrate formation) should be taken into account in Kohler model calculations of hygroscopic growth and CCN activation.

35 First, if the dehydration processes (efflorescence, restructuring, or desorption) inside DMA are completed within 0.1 s, then the resulting changes in particle mobility diameter should be fully captured with deviations $<1\%$. And also, kinetically limited dehydration processes that lead to progressive changes of particle mobility on a time scale of 0.1–10 s should significantly influence the particle sizing (deviations $>1\%$) and lead to a broadening of the measured size distributions. Dehydration processes progressing on time scales >10 s should have no effect on particle sizing (no change of mobility diameter and no broadening of size distribution).

40 Thanks for your explanation. I agree that void fractions and residual water should be taken into account; however, how can you do this with the measurements you have made?

Here is how I would proceed: You are making the assumption that drying imposed by the nafion, and by the dry sheath air inside the DMA, are sufficient to remove water associated with the ambient particles. Why not state this assumption, and move on without reference to "kinetic

limitations” or Mikhailov et al. (2009)?

Re: Yes, you are correct, and your statement is exactly our assumption. Thank you! It has been revised (see Page 7, lines 107-108).

P16147L25

5 It is the inner diameter, not the outer diameter, that is relevant.

Re: it is just the outer diameter.

It’s the inner diameter that is important. Please report that value.

Re: The inner diameter is 0.38 inch. (Revised)

P16148L19

10 “.temperature stability was zero.” I don’t understand what you are referring to here.

Re: here it means the data is invalid if the “temperature stability” was flagged as “0”. And for the valid data, the “temperature stability” was flagged as “1”. The sentence has been revised.

Thanks for your explanation. Why can’t you explain what is meant by “stability”? Isn’t this the average difference between what is preset and what is measured?

15 Re: sorry for not explaining it clearly. But you’ve got the point. The “temperature stability” refers to the T_1 , T_2 and T_3 in cloud chamber of the CCNc, which is set to obtain the target supersaturations. If the average differences between preset T_1 , T_2 and T_3 and the measured values are larger than $0.4\text{ }^\circ\text{C}$, the “temperature stability” is flagged as “0”. Thus, the data is invalid and will be removed. This has been revised in the paper(see Page 9, lines 150-153)

20

P16148L21

Here you define the “aerosol number (CN) size distribution spectrum.” How is this different from the PSD mentioned on P16147L1 and on P16148L24?

25 Re: that’s exactly the same thing. We have corrected all of them to particle number size distribution in the revised paper.

PSDs are shown in Figure 2 (revision). It is not clear how the quantity on the Y axis, once integrated over all sizes, becomes the CN concentration referred to in the text. For example, on L241 we are told that the CN concentration is $\sim 1.7 \times 10^4\text{ cm}^{-3}$. Typically in aerosol science the PSD is $dN/d\log D$ and the latter has dimension cm^{-3} . How are we to interpret the “N” on the Y axis of Figures 2a-c? For an example see here in their Figure 12a (Atmos. Chem. Phys., 13, 7263–7278, 2013).

30

Re: Thanks for pointing this. It should be $dN/d\log D\text{ (cm}^{-3}\text{)}$ in Figure 2. The figures have been revised. (see Figure 2)

35 P16152L6

It is the “CCN activity”, not the “aerosol activity”, that is the focus here.

Re: corrected.

Please see L227 in the revision. This was not “corrected.” If you do not feel the correction is needed, just say so in your response.

40 Re: sorry for my carelessness, I agree your suggestion. It has been corrected in the revision. (see Page 13, line 241)

P16153L26

Here is a relevant reference.

Snider, J.R., and, S.Guibert, J.-L. Brenguier and J.-P.Putaud, Aerosol activation in marine stratocumulus clouds: Part – II Köhler and parcel theory closure studies, *J. Geophys. Res.*, 108, doi:10.1029/2002JD002692, 2003

5 Re: the reference has been added.

I see this paper in the References, but I do not see it cited in the text.

Re: Added it this time. (Page 4, line 27)

P15154L7

10 What are “bulk ARs”?

Re: bulk ARs means the ratio of NCCN to NCN, which is calculated from the total CN and CCN number concentrations. Thus, we called it bulk ARs. For the size-resolved CCN measurements, we can get size-resolved ARs from size-resolved CCN and CN number concentrations.

15 Thanks for your explanation; however, what you wrote (revision) needs to be removed from the middle of the paragraph that discusses the size-resolved AR. I recommend that the removed text be put somewhere else (e.g., at the end of the paragraph). For example, on L52, you could state: “The bulk activation ratio (bulk AR) is defined as the CCN-measured concentration divided by the CN concentration. These values were measured in ambient air, every ?? minutes, and without particle size selection in the DMA.”

20 Re: Thanks a lot for your comments. In this revision, this has been revised as follows (also see Page 10, lines 161-166),

25 “The size-resolved CCN activation ratio (size-resolved AR) is defined as the $dN_{CCN}/d\log D_p$ divided by the $dN_{CN}/d\log D_p$. These values were measured by SMPS-DMT-CCNc with particle size selection in the DMA. The bulk activation ratio (bulk AR) is defined as the total CCN concentration divided by the total CN concentration. The total CCN and CN number concentrations are integrated by the measured CCN and CN size distribution respectively over the whole size range.”

P16155L2 What you are calling the “estimate” is the summed product of AR(D) and PSD(D)? Right? 30 By “Observation” you are talking about the direct measurement of the ambient $N_{ccn}(S)$ made _without_ the DMA in front of the CCN instrument. I did not see mention of the ambient $N_{ccn}(S)$ measurement (without the DMA in front) in Section 2.1.

35 Re: We used a Scanning Mobility Particle Sizer (SMPS), combined with a Droplet Measurement Technologies-Cloud Condensation Nuclei Counter (DMT-CCNc) (Lance et al., 2006), for size-resolved CCN measurements as well as particle number size distribution (PSD) measurements. The SMPS is just the DMA.

To estimate NCCN, estimated CCN size distributions at the five supersaturations were calculated by multiplying the campaign-averaged CCN efficiency spectrum with the actually measured PSD. The estimated NCCN at the five supersaturations was then calculated by integrating the estimated CCN size distribution over the whole size range. The measured CCN size distributions are integrated to produce the observed NCCN. 40

Thanks for the explanation. In the revision, do you explain what you mean by the “observed NCCN”?

Re: Yes. This has also been explained in the text. (see Page 16, lines 321-328; Page 18, lines

376-379)

P16155L19

I would reword this because the Figure 7 shows how the difference (estimated minus observed) varies with chi-org. The latter is the independent variable. There are other places in the manuscript where “sensitivity” is used. I would change the word order in some of these instances too. E.g., P16145L26. There are other places too.

Re: revised. Because in the revised version, the sensitivity of oxidation level (using f44, the fraction of m/z 44 in total organics, as an indicator) of organics to estimation of NCCN is also examined. The section is thus rewritten (see Section 4.4, and Figure 5 and Figure 6).

In my opinion this argument is presented backwards, both in the original manuscript, and in the revision.

Here is an example from the abstract (revised):

“The sensitivity of volume fraction of organic aerosols (chi-org) as well as oxidation level (using f44, the fraction m/z 44 in total organics, as an indicator) of organics on estimating NCCN is examined.”

I feel that the authors should reword these statements. Here is a suggested replacement sentence for the sentence above:

“The sensitivity of the estimated CCN number concentration (NCCN) to both volume fraction of organic material (chi-org) and aerosol oxidation level (using f44, the fraction m/z 44 in aerosol organic material) are examined.”

Re: thank you very much for correcting the presentation regarding to this part. We totally agree to your comments and correction. That has been revised carefully (see Page 2, lines 2-5)

Another example is seen on L65 (revision). Going back to what I said in my first review, I feel that the authors should be focused on how NCCN is sensitive to aerosol chemical composition, not the other way around.

Re: revised as “...The aim of this paper is to examine the sensitivity of CCN activity to aerosol physicochemical properties (especially aerosols containing large amounts of organics, as well as the oxidation level)...” (see pages 6, lines 66-68)

Another example is L294 (revision).

Re: revised as “...we examine the sensitivity of N_{CCN} to both volume fraction of organics (x_{org}) and oxidation or aging of organics based on measurement at Xinzhou site...” (see Page 16, lines 307-309)

Another example is the caption of Figure 5 (revision).

Re: revised as “...The sensitivity of N_{CCN} to both organics volume fraction (x_{org}) and oxidation level (using f_{44} , the fraction of m/z 44 in aerosol organic material) of organics at supersaturation levels of” (see the caption of Figure 5)

Another example is L396 (revision)

Re: revised as “...we examine the sensitivity of N_{CCN} to both volume fraction of organics (x_{org}) and oxidation or aging of organics based on measurement at Xinzhou site.” (see Page 20, lines 409-412)

Additional comments:

According to Petters et al. (ACP, 2007), the kappa for ammonium sulfate is 0.61 and the kappa for

ammonium nitrate is 0.67 (see their Table 1; CCN derived kappa). Hence, the sentence on L181 (revision) is backwards.

Re: revised. Thanks a lot for your careful check.

L117 (revision) – here you are referring to the “overall relative error”

5 Re: corrected. Thank you very much.

L275 (revision) – The sentence needs work (....“it should be caution”)

Re: revised. (Page 15, lines 289-290)

L345 (revision) – misspelled word “usully”

Re: corrected.

10 L388 (revision) – This mentions “local primary biomass burning” but I do not see discussion of the topic in the analysis section of the manuscript.

Re: revised as “...CCN efficiency was largely reduced by local air masses...” (see Page 19, line 401)

General – if the subscript is “org” for chi, it should also be “org” for epsilon (i.e., not “Org”).

Re: corrected.

15

20 **Impacts of organic aerosols and its oxidation level on CCN activity from measurement at a suburban site in China**

Fang Zhang^{1,2}, Zhanqing Li^{*1,2,3}, Yanan Li^{1,2}, Yele Sun⁴, Zhenzhu Wang⁵, Ping Li^{1,2},

Li Sun⁶, Maureen Cribb³, Chuanfeng Zhao^{1,2}, Qingqing Wang⁴

¹State Key Laboratory of Earth Surface Processes and Resource Ecology, College of Global Change and Earth System Science, Beijing Normal University, Beijing 100875, China

25

²Joint Center for Global Change Studies, Beijing 100875, China

³Earth System Science Interdisciplinary Center and Department of Atmospheric and Oceanic Science, University of Maryland, College Park, Maryland, USA.

⁴State Key Laboratory of Atmospheric Boundary Layer Physics and Atmospheric Chemistry, Institute of Atmospheric Physics, Chinese Academy of Sciences, Beijing 100029, China

30

⁵Key Laboratory of Atmospheric Composition and Optical Radiation, Anhui Institute of Optics and Fine Mechanics, Chinese Academy of Sciences, Hefei 230031, China

⁶Liaoning Weather Modification Office, Shenyang, 112000, China

35

***correspondence to: Z. Li (zli@atmos.umd.edu)**

Abstract

This study is concerned with the impacts of organic aerosols on CCN activity based on field measurements made at a suburban site in north China. The sensitivity of the estimated CCN number concentration (N_{CCN}) to both volume fraction of organic aerosol material (x_{org}) as well as aerosol oxidation level (using f_{44} , the fraction of m/z 44 in total organics, as an indicator) of organics on estimating N_{CCN} is examined. A strong dependence of CCN number concentration (N_{CCN}) on the x_{org} and f_{44} was noted. The sensitivity of volume fraction of organics to N_{CCN} increased with increasing x_{org} . The impacts of the aerosol particles oxidization or aging level on estimating N_{CCN} were also very significant. When the particles were mostly composed of organics ($x_{org}>60\%$), the N_{CCN} at the supersaturation of 0.075% and 0.13% was underestimated by 46% and 44% respectively if aerosol particles were freshly emitted with primary organics ($f_{44}<11\%$); while the underestimation decreased to 32% and 23% at the corresponding supersaturations if the particles were with more hygroscopic secondary organics ($f_{44}>15\%$). The N_{CCN} at the supersaturation of 0.76% was underestimated by 11% and 4% respectively at $f_{44}<11\%$ and $f_{44}>15\%$. But for the particles composed of low organics (e.g. $x_{org}<40\%$), the effect caused by the f_{44} was quite insignificant both at high and low supersaturations. This is due to that the overall hygroscopicity of the particles is dominated by inorganics such as sulfate and nitrate, which are more hygroscopic than organic compounds. Our results indicated that it would decrease the uncertainties in estimating N_{CCN} and lead to a more accurate estimation of N_{CCN} to

带格式的

带格式的

带格式的

带格式的

带格式的

带格式的

increase the proportion of secondary organics, especially when the composition of the aerosols is dominated by organics.

The applicability of the CCN activation spectrum obtained at Xinzhou to the Xianghe site, about 400 km to the northeast of Xinzhou, was investigated, with the
5 | aim of further examining the sensitivity of $\epsilon_{\text{CCN}} N_{\text{CCN}}$ to aerosol type. Overall, the mean CCN efficiency spectrum derived from Xinzhou performs well at Xianghe when the supersaturation levels are $> 0.2\%$ (overestimation of 2-4%). However, N_{CCN} was overestimated by $\sim 20\%$ at supersaturation levels of $< 0.1\%$. This suggests that the overestimation is mainly due to the smaller proportion of aged and oxidized organic
10 | aerosols present at Xianghe compared with Xinzhou.

11 1. Introduction

12 To reduce the uncertainty of aerosol indirect effects on the radiative balance of
13 the atmosphere, it is important to gain a good knowledge of the ability of aerosol
14 particles to form cloud condensation nuclei (CCN) at the typical supersaturations
15 found in the atmosphere. The CCN activity of aerosol particles is governed by the
16 Köhler theory (Köhler, 1936). This theory determines CCN from aerosol particle size
17 and physicochemical properties, which include the molar volume, activity coefficient,
18 and effect on surface tension (McFiggans et al., 2006). These properties, however, are
19 difficult to measure.

20 Researchers have proposed single-parameter models to parameterize the CCN
21 activation and hygroscopicity of multi-component aerosols (Hudson and Da, 1996;
22 Rissler et al., 2006; Petters and Kreidenweis, 2007; Wex et al., 2007). Field
23 experiments have been conducted with the aim of better characterizing particle
24 physicochemical parameters influencing cloud CCN activation. Due to the large
25 spatial variability of aerosol types and compositions, the CCN activation efficiency
26 varies greatly over different regions. CCN number concentrations (N_{CCN}) can often be
27 better predicted in the background atmosphere (Chuang et al., 2000; Dusek et al.,
28 2003; VanReken et al., 2003; Snider et al., 2003; Rissler et al., 2004; Gasparini et al.,
29 2006; Stroud et al., 2007; Bougiatioti et al., 2009).

30 The largest errors are associated with urban emissions (Sotiropoulou et al., 2007).
31 This is likely due to the organics component of aerosol particles, which have the
32 largest uncertainty and are not fully understood. Biomass burning aerosols and
33 secondary organics formed from the oxidation of common biogenic emissions are
34 often more difficult to activate (Mircea et al., 2005; VanReken et al., 2005; Lee et al.,
35 2006; Varutbangkul et al., 2006; Clarke et al., 2007; Rose et al., 2010; Engelhart et al.,

2012; Paramonov et al., 2013; Latham et al., 2013; Mei et al., 2013b; Zhang et al., 2014). Particles with aged/oxidized secondary organic components (e.g., organic acids) have been shown to be more hygroscopic (Raymond and Pandis, 2002; Hartz et al., 2006; Bougiatioti et al., 2011), but still much less hygroscopic than inorganic species. The sensitivity of estimated N_{CCN} to organics have been examined in a number of recent studies (Wang et al., 2008; Reutter et al., 2009; Ervens et al., 2010; Kammermann et al., 2010; Ward et al., 2010; Zhang et al., 2012; Mei et al., 2013a). It is widely known that the estimated N_{CCN} is sensitive to changes in organics due to the latter's complex components. The amounts and hygroscopicity parameter of organics (κ_{org}) vary substantially and lead to significant biases in estimating CCN concentrations and aerosol indirect forcing (Sotiropoulou et al., 2007; Hings et al., 2008; Liu and Wang, 2010). Therefore, field investigations regarding CCN activity and organics impacts, especially in heavily polluted regions, are pivotal to better parameterize CCN in climate models.

Northern China is a fast developing and densely populated region of China, where aerosol loading is high (Li et al., 2007, 2011), the particle composition is complex, and severe haze pollution episodes are common (Guo et al., 2014). In recent years, CCN measurements have been collected during field campaigns carried out in the region (Wiedensohler et al., 2009; Gunthe et al., 2011; Yue et al., 2011; Deng et al., 2011, 2013; Zhang et al., 2014). These studies have presented different perspectives on the influence of particle size and composition on CCN activity. For example, Deng et al. (2013) evaluated various schemes for CCN parameterization and recommended that the particle number size distribution (PSD) together with inferred mean size-resolved activation ratios can be used to estimate CCN number concentrations without considering the impact of particle composition. However,

61 Zhang et al. (2014) demonstrated that the 30–40% uncertainties in N_{CCN} are mainly
62 associated with changes in particle composition. None of the above-mentioned studies
63 have investigated the impact of organics on estimating N_{CCN} in Northern China.
64 Zhang et al. (2012) noted a more significant influence of organics on CCN activity but
65 without concerning the influences of particles oxidation or aging on CCN activity; in
66 addition, the campaign average mass fraction of organics in their study was $< 20\%$.

67 The aim of this paper is to examine the sensitivity of ~~changes in~~ CCN activity to
68 aerosol physicochemical properties (especially aerosols containing large amounts of
69 organics, as well as the oxidation level) ~~to CCN activity,~~ and also to see how much
70 uncertainty is incurred by applying the CCN efficiency spectra measured at one site to
71 another site in a heavily polluted region. The instrumentation and data used in the
72 study are described in section 2. The method for calculating the hygroscopicity
73 parameter (κ_{chem}) is introduced in section 3. The sensitivity of x_{org} as well as oxidation
74 level of organics on estimating N_{CCN} in section 4, and the ability of the CCN
75 efficiency spectrum observed at the Xinzhou site to represent CCN at the Xianghe site,
76 are also presented and discussed at the last part of this section. Conclusions from the
77 study are given in section 5.

78 2. Measurements and data

79 An intensive observation period field campaign similar to the
80 Aerosol-CCN-Cloud Closure Experiment (Zhang et al., 2014), called the Atmosphere,
81 Aerosol, Cloud, and CCN (A²C²) experiment, was conducted from 22 July to 26
82 August of 2014 at Xinzhou (38.24°N, 112.43°E; 1500 m above sea level), a city with a
83 population of 0.51 million in Northern China. The site is located about 360 km
84 southwest of the metropolitan Beijing area and about 10 km south of the local town
85 center. The site is surrounded by agricultural land (e.g., corn) with little local pollution

86 plums from motor vehicles and industrial activities. Sitting between two mountains
87 (Taihang Mountain to the east and Lüliang Mountain to the west), the site also
88 experiences air masses from Xinzhou City to the north and from Taiyuan City to the
89 south, the capital of Shanxi Province. Air masses from the northeast and southwest
90 dominate over the site during summer. Depending on the wind direction,
91 measurements at the Xinzhou site can detect air parcels of urban, rural, or mixed
92 origins, including both fresh biogenic emissions around the site and aged aerosols
93 from advection.

94 **2.1 Instruments and measurements**

95 During the field campaign, a Scanning Mobility Particle Sizer (SMPS),
96 combined with a Droplet Measurement Technologies-Cloud Condensation Nuclei
97 Counter (DMT-CCN_c) (Lance et al., 2006), was used for size-resolved CCN
98 measurements as well as particle number size distribution (PSD) measurements. The
99 measured aerosol PSD is within the size range of 14-600 nm. Aerosol chemical
100 composition was measured simultaneously by an Aerodyne Aerosol Chemical
101 Speciation Monitor (ACSM) (Sun et al., 2012).

102 The aerosol inlet for the size distribution measurements was equipped with a TSI
103 Environmental Sampling System (Model 3031200), which consists of a sharp-cut
104 PM₁ cyclone and a bundled nafion dryer. The size-resolved CCN efficiency spectra
105 were measured by coupling the DMT-CCN_c used with the SMPS (Rose et al., 2008).
106 In this step, the particles are rapidly dried with RH < 30% upon entering the
107 Differential Mobility Analyzer (DMA). Thus, size selection is effectively performed
108 under dry conditions. The nafion dryer and the sheath air inside the DMA are
109 sufficient to remove residual water associated with the ambient particles. Relative

110 | deviations in particle diameter should be $< 1\%$ ~~except for potential kinetic limitations~~
111 | ~~(Mikhailov et al., 2009).~~%. The sample flow exiting the DMA was split into two parts:
112 | 0.3 lpm for the CPC and 0.5 lpm for the CCN counter (CCN_C). The DMA, controlled
113 | by TSI-AIM software, scanned one size distribution every five minutes. The CCN_C
114 | was operated at a total flow rate of 0.5 lpm with a sheath-to-aerosol flow ratio of 10.
115 | The inlet RH for CCN_C was $< 30\%$. During the field campaign, the mean sample
116 | temperature and pressure measured by CCN_C sensors was $(24.3 \pm 1.4)^\circ\text{C}$ and
117 | (898.4 ± 11.7) hPa. The supersaturations levels of CCN_C were calibrated with
118 | ammonium sulfate before and after the field campaign, following the procedures
119 | outlined in Rose et al. (2008). During each CCN measurement cycle, calibrated
120 | effective supersaturations were set at 0.075%, 0.13%, 0.17%, 0.39%, and 0.75%. The
121 | overall relative error (1σ) for the supersaturation levels was estimated to be $< 3.5\%$.
122 | The completion of a full measurement cycle took 50 minutes (10 minutes for each
123 | supersaturation level).

124 | The measurement of non-refractory submicron aerosol species including
125 | organics, sulfate, nitrate, ammonium, and chloride were made with an ACSM. During
126 | the field campaign, ambient aerosols were drawn inside through a $\frac{1}{2}$ inch (outer
127 | diameter, the inner diameter is 0.38 inch) stainless steel tube at a flow rate of ~ 3 L
128 | min^{-1} , of which ~ 84 cc min^{-1} was sub-sampled into the ACSM. An URG cyclone
129 | (Model: URG-2000-30ED) was also positioned in front of the sampling inlet to
130 | remove coarse particles with a cut-off size of 2.5 μm . Before sampling into the ACSM,
131 | aerosol particles were dried using a silica gel desiccant. The residence time in the
132 | sampling tube was ~ 5 s. The ACSM was operated at a time resolution of ~ 15 min with
133 | a scan rate of mass spectrometer at 500 ms amu^{-1} from m/z 10 to 150. Regarding the
134 | calibration of the ACSM, mono-dispersed, size-selected 300-nm ammonium nitrate

135 particles within a range of concentrations were sampled into both the ACSM and a
136 condensation particle counter (CPC). The ionization efficiency (IE) was then
137 determined by comparing the response factors of the ACSM to the mass calculated
138 with known particle size and number concentrations from the CPC. More detailed
139 descriptions of the operation and calibration of the ACSM are given in Sun et al.
140 (2012) and Ng et al. (2011). The campaign averaged mass concentration of PM_{10} is
141 $31.6 \mu\text{g m}^{-3}$.

142 In addition to the ACSM, the black carbon (BC) in $PM_{2.5}$ was simultaneously
143 measured at a time resolution of 5 min by a seven-wavelength aethalometer (Model
144 AE31, Magee Scientific Corporation). The campaign averaged mass concentration of
145 BC is $\sim 2.5 \mu\text{g m}^{-3}$. During the experiment, the campaign area was generally hot and
146 dry, with an average temperature of $21.6 \text{ }^\circ\text{C}$ and an average ambient RH of 69.5%.

147 2.2 Data

148 The raw CCN data were first filtered according to instrument recorded
149 parameters (e.g., temperature and flow). For example, if the relative difference
150 between the actual and preset sample flows was larger than 4%, the data are flagged
151 as invalid. The data is also excluded if the “temperature stability” was flagged as “0”.

152 ~~These flagged data are not used for further analysis.~~ Here, the “temperature stability”
153 refers to the T_1 , T_2 and T_3 in cloud chamber of the CCNc, which is set to obtain the
154 target supersaturations. If the average differences between preset T_1 , T_2 and T_3 and the
155 measured values are larger than $0.4 \text{ }^\circ\text{C}$, the “temperature stability” is flagged as “0”.

156 Thus, the data is invalid and will be removed. A multiple charge correction and
157 transfer function (Deng et al., 2011) is applied to each PSD as well as to the CCN
158 efficiency spectrum. ~~The CCN activation ratio (AR) is the ratio of N_{CCN} to CN~~

带格式的

159 concentration (N_{CN}). Bulk AR is calculated from the total N_{CN} and N_{CCN} . For the
160 size-resolved CCN measurements, we get size-resolved AR from size-resolved CCN
161 and CN number concentrations.

162 —Size-resolved CCN and PSD data, measured with a DMT-CCNc and a
163 SMPS (with a particle size range of 10-700 nm) on 7-21 July 2013 at Xianghe (Zhang
164 et al., 2014), are used in this study for comparisons with CCN activity at the Xinzhou
165 site. Aerosol mass concentrations were processed using the ACSM standard data
166 analysis software (version 1.5.3.0). Detailed procedures for the data analysis have
167 been described by Ng et al. (2011) and Sun et al. (2012). The size-resolved CCN
168 activation ratio (size-resolved AR) is defined as the $dN_{CCN}/d\log D_p$ divided by the
169 $dN_{CN}/d\log D_p$. These values were measured by SMPS-DMT-CCNc with particle size
170 selection in the DMA. The bulk activation ratio (bulk AR) is defined as the total CCN
171 concentration divided by the total CN concentration. The total CCN and CN number
172 concentrations are integrated by the measured CCN and CN size distribution
173 respectively over the whole size range.

174 3. Derivation of κ_{chem}

175 In this study, we calculate κ_{chem} based on bulk chemical composition observations
176 made during the field campaign. The method is very similar to that used by Zhang et
177 al., (2014). As proposed by Petters and Kreidenweis (2007), κ_{chem} can be predicted
178 using a simple mixing rule based on chemical volume fractions for a given internal
179 mixture:

$$180 \quad \kappa_{chem} = \sum_i \varepsilon_i \kappa_i \quad (1)$$

181 where κ_i and ε_i are the hygroscopicity parameter and volume fraction, respectively, for
182 the individual (dry) components in the mixture and i is the number of components in
183 the mixture.

184 Measurements from the ACSM in Xinzhou show that the composition of
 185 submicron particles was dominated by organics, followed by sulfate, ammonium, and
 186 nitrate. The contribution of chloride was negligible (volume fraction of about < 2%).
 187 The analysis of the anion and cation balance suggests that anionic species (NO_3^- ,
 188 SO_4^{2-}) were essentially neutralized by NH_4^+ over the relevant size range. For
 189 refractory species, BC represented a negligible fraction of the total submicron aerosol
 190 volume (< 3%). Sea salt and dust are usually coarse mode particles with particle sizes >
 191 $1 \mu\text{m}$ (Whitby, 1978). The contribution of such types of aerosols is thus expected to be
 192 negligible for sizes < $1 \mu\text{m}$. Therefore, the submicron particles measured by the ACSM
 193 mainly consisted of organics, $(\text{NH}_4)_2\text{SO}_4$, and NH_4NO_3 . The particle hygroscopicity is
 194 thus the volume average of the three participating species:

$$195 \quad \kappa_{chem} = \kappa_{org} \varepsilon_{org} = \kappa_{org} \varepsilon_{org} + \kappa_{(\text{NH}_4)_2\text{SO}_4} \varepsilon_{(\text{NH}_4)_2\text{SO}_4} + \kappa_{\text{NH}_4\text{NO}_3} \varepsilon_{\text{NH}_4\text{NO}_3} \quad (2)$$

196 Here, the values of κ for $(\text{NH}_4)_2\text{SO}_4$ and NH_4NO_3 are 0.6761 and 0.6167,
 197 respectively. The following linear function derived by Mei et al. (2013) was used to
 198 estimate κ_{org} in this study: $\kappa_{org} = 2.10 \times f_{44} - 0.11$, where f_{44} is the fraction of m/z
 199 44 in total organics. The mean value of κ_{org} during the field campaign is
 200 0.115 ± 0.019 .

201 4. Results and discussion

202 4.1 CCN efficiency spectra

203 During the field campaign at the Xinzhou site, ~790 size-resolved CCN
 204 efficiency spectra at five supersaturation levels ranging from 0.075% to 0.76% were
 205 measured. Figure 1 shows campaign averaged spectra of the measured CCN
 206 efficiency at Xinzhou for supersaturation levels of 0.075%, 0.13%, 0.17%, 0.39%, and
 207 0.76%. The observed averaged CCN efficiency spectra during Xianghe campaign in

208 summer 2013 are also shown. The Note that the maximum activation fraction (MAF)
209 for Xianghe site showed in Figure 1 is slight lower than that we plotted in Zhang et
210 al.(2014). Because some data points when the MAF value >1 were not processed
211 previously, as resulted in larger mean MAF. But in this paper, the data points with
212 $MAF > 1.0$ were forced to 1 when $D_p > 300$ nm, which could be completely activated
213 at even lower supersaturations but the MAF would never be larger than 1.0. In Figure
214 1, the right panels show the mass concentration fraction of particle chemical
215 compositions at Xinzhou (top panel) and Xianghe (bottom panel) during their
216 respective observation periods. Significant differences in size-resolved CCN
217 efficiency spectra at the two sites are seen. Aerosol particles at Xinzhou activate more
218 efficiently (higher values of AR) at a given particle diameter (D_p) for the same
219 supersaturation level. In the other words, a larger D_p was required to reach the same
220 activation efficiency at Xianghe. This suggests that aerosol properties at each site
221 differ.

222 The slope of AR with respect to diameters near D_p when AR=50% (defined here
223 as the cut-off diameter, D_{cut}) provides information about the heterogeneity of the
224 composition for size-resolved particles. For an ideal case when all CCN-active
225 particles have the same composition and size, a steep change in AR from 0 to 1 would
226 be observed as D_p reached D_{cut} . A gradual increase in size-resolved AR with D_p
227 suggests that aerosol particles have different hygroscopicities. The steeper slopes of
228 AR around D_{cut} observed at Xinzhou suggest that the particle composition was less
229 heterogeneous with more hygroscopicity than particles at the Xianghe site. This can
230 be partially explained by the magnitudes of the mean κ_{chem} at the two sites (0.42 at
231 Xinzhou and 0.38 at Xianghe). Also, the f_{44} is greater at Xinzhou than at Xianghe. The
232 m/z 44 signal is mostly due to acids (Takegawa et al., 2007; Duplissy et al., 2011) or

233 acid-derived species, such as esters. f_{44} is closely related to the organic oxidation level
234 (Aiken et al., 2008). Oxidized/aged acids are generally more hygroscopic and easily
235 activated. Moreover, the primary inorganic particles at the Xinzhou site are sulfates,
236 with a mass fraction that is two times greater than that measured at Xianghe.
237 Therefore, particles at the Xinzhou site consist of more hygroscopic sulfate-dominant
238 inorganics and aged/oxidized secondary organics and can thus be more efficiently
239 activated at a given D_p , as shown in Fig. 1.

240 4.2 Air mass influences on CCN activity: a case study

241 Because air mass back trajectories combined with ambient air measurements can
242 be used for analyzing large-scale air pollutant transport and source identification at a
243 receptor site (Stohl, 1996; Rousseau et al., 2004), in this study, we calculated five-day
244 (120 hr) back trajectories using the Hybrid Single-Particle Lagrangian Integrated
245 Trajectory (HYSPLIT) model (Draxler and Hess, 1998) with National Centers for
246 Environmental Prediction (NCEP) reanalysis data. TrajStat software (Wang et al.,
247 2009) has been used to calculate trajectories. The arrival height of the trajectories at
248 the Xinzhou site was at the surface.

249 Three cases were selected to study air mass influences on aerosol-CCN activity:
250 (1) Case 1, 19 August 2014, 19:00-21:00 local time (LT); (2) Case 2, 9 August 2014,
251 03:00-10:00 LT; and (3) Case 3, 29 July 2014, 00:00-12:00 LT. Each case is
252 associated with a different CCN efficiency spectrum, i.e., top, middle, and bottom
253 panels of Fig. 2 are for Cases 1, 2, and 3, respectively. Their respective back
254 trajectories are shown in Fig. 3.

255 In Case 1, air trajectories (red line in Fig. 3) originated from the southwest and
256 passed through northern Shaanxi Province and northwestern Shanxi Province, then

257 rounded back to the site from the north/northeast. So, aerosols in this case are closely
258 associated with air parcels north/northeast of the site. The trajectories were very short,
259 suggesting that the air flow was slow during the observational period. Under these
260 circumstances, aerosol loading would be largely impacted by local sources around the
261 site. A high mass fraction of organics ($> 60\%$) with low f_{44} ($\sim 10\%$) and κ_{chem} (< 0.3)
262 values was measured during the observational period. Furthermore, the PSD showed
263 one peak mode with $D_p = 56$ nm and a high N_{CN} ($\sim 1.7 \times 10^4$ cm $^{-3}$), but low mass
264 concentration of PM_{10} (28.36 $\mu\text{g m}^{-3}$). This suggests that particles may be composed of
265 freshly emitted primary aerosols (the biogenic emissions from the plants and trees
266 around the site). This type of aerosol is usually less hygroscopic with a single peak
267 mode primarily composed of fine particles (Whitby, 1978; Hussein et al., 2005).
268 These aerosols cannot activate efficiently. The maximum activation fraction (MAF)
269 shown in the top right panel of Fig. 2 is less than 0.6 at all supersaturation levels for
270 particles with $D_p > 300$ nm, indicating that the particles should be largely externally
271 mixed aerosols.

272 In Case 2 (blue line in Fig. 3), air parcels moved rapidly from the west to the site.
273 The site should then be influenced by the large-scale transport of air masses. For this
274 case, aerosols contain a small amount of organics ($< 30\%$), but have high f_{44} ($\sim 14\%$)
275 and κ_{chem} values (~ 0.5). The PSD showed a double peak mode with an N_{CN} of
276 $\sim 1.3 \times 10^4$ cm $^{-3}$ and a relatively high mass concentration of PM_{10} (81.45 $\mu\text{g m}^{-3}$). The
277 double peak mode suggests that aerosols in this case are a mixture of aerosols from
278 local sources and from other regions (Whitby, 1978; Dal Maso et al., 2007). Because
279 aerosols are aged and oxidized during long-distance transport, these particles are
280 usually composed of secondary organic and inorganic components with more
281 hygroscopicity (Weber et al., 1999; Verver et al., 2000). These aerosols can activate

282 efficiently. The MAF is close to 1 and the slopes of AR around D_{cut} are steep at all
283 supersaturation levels (middle right panel of Fig. 2). This CCN efficiency spectrum is
284 similar to the ideal spectrum of pure ammonium sulfate.

285 In Case 3 (green line in Fig. 3), air parcels travelled from the northwest to the
286 site. Air masses arriving at the site in this case had passed over densely populated
287 regions with more heavy pollution. A gradual increase in size-resolved AR with D_p is
288 seen (bottom right panel of Fig. 2). This is attributed to the diversity in aerosol
289 hygroscopicity because of the complex nature of the chemical composition of aerosol
290 particles.

291 4.3 Correlation of N_{CN} and N_{CCN}

292 Figure 4 shows N_{CN} as a function of N_{CCN} for different supersaturation levels at
293 the Xinzhou and Xianghe sites. They showed high or moderate correlations at high
294 supersaturation levels (e.g., $R^2 = 0.57$ at Xinzhou and $R^2 = 0.85$ at Xianghe at a
295 supersaturation level of $\sim 0.8\%$), but quite poor correlations at low supersaturation
296 levels. Although [Andreae \(2009\)](#) proposed using the relationship of CCN and CN, or
297 even aerosol optical depth (AOD), to parameterize CCN in models, it ~~should be~~
298 ~~caution if one uses the correlation would lead to large uncertainties especially for those~~
299 ~~eases at low when the supersaturations because of the spatial variation in CCN~~
300 ~~activity for maritime and continental aerosols are low.~~ It was noticed that there was an
301 apparent higher degree of correlation at Xianghe site for each supersaturation than
302 that derived at Xinzhou site. In view of the similar regimes from which the data are taken
303 and the same instruments by which they have been collected, the discrepancy between
304 Xianghe and Xinzhou should be caused largely by the spatial variations of aerosols types.
305 These variations are primarily attributed to variations in aerosol particle size, i.e., the
306 shape of the PSD as well as particle composition. As presented by [Zhang et al. \(2014\)](#),

307 the relationship between bulk activation ratios and N_{CCN} was complex under polluted
308 conditions and was heavily dependent on the physicochemical properties of
309 atmospheric aerosols.

310 **4.4 Impact of x_{org} on N_{CCN}**

311 Precise quantification of N_{CCN} is crucial for understanding aerosol indirect
312 effects and characterizing these effects in models. A CCN closure study is useful to
313 examine the controlling physical and chemical factors and to help verify experimental
314 results. N_{CCN} is usually derived from measured aerosol properties, such as PSD and
315 composition or hygroscopicity based on the Köhler theory. Achieving such closure
316 under heavily polluted conditions is more challenging, especially due to the complex
317 effects of organics on CCN activity. In this section, we examine the sensitivity of
318 N_{CCN} to both volume fraction of organics (x_{org}) as well as and oxidation or aging of
319 organics to N_{CCN} estimation based on measurement at Xinzhou site. During the
320 observed period, aerosols at the Xinzhou site were dominated by organics, with 12%, 23%,
321 39%, and 25% of the data points corresponding to $x_{\text{org}} > 60\%$, $50\% < x_{\text{org}} < 60\%$, $40\% < x_{\text{org}}$
322 $< 50\%$ and $x_{\text{org}} < 40\%$, respectively. For the purpose of examining the sensitivity of
323 estimated N_{CCN} to x_{org} and oxidation/aging level, we sorted the size-resolved CCN
324 data when the $x_{\text{org}} > 60\%$, $50\% < x_{\text{org}} < 60\%$, $40\% < x_{\text{org}} < 50\%$ and $x_{\text{org}} < 40\%$. Furthermore,
325 for each level of x_{org} , we tested the impacts on N_{CCN} estimation both from the most
326 oxidized (with f_{44} of higher than 15%) and least oxidized (those primary organic
327 aerosols with f_{44} of lower than 11%) organic particles. For example, the size-resolved
328 CCN data points during the period when $x_{\text{org}} > 60\%$ and also $f_{44} > 15\%$ was averaged to
329 generate the averaged CCN efficiency spectra at the five supersaturations respectively.
330 Then we used the produced averaged CCN efficiency spectra to estimate N_{CCN} .

331 Estimated CCN size distributions at the five supersaturations were firstly
332 calculated by multiplying the averaged CCN efficiency spectrum (by using the
333 averaged CCN efficiency spectra, the aerosol particles were assumed with uniform
334 chemical composition without considering the effects of the temporal variations of the
335 activation curves on CCN activity) with the actually measured PSD. Then, we
336 integrated the estimated CCN size distribution over the whole size range to generate
337 estimated N_{CCN} . While the measured CCN size distributions are integrated to produce
338 the observed N_{CCN} .

339 Observed and estimated N_{CCN} at four supersaturation levels (0.075%, 0.13, 0.17
340 and 0.76%) were showed in Fig 5. The data points presented more disperse and
341 weaker correlations at lower supersaturations. The sensitivity of volume fraction of
342 organics to N_{CCN} increased with increasing x_{org} . This is especially for the case of these
343 primary organic particles with $f_{44} < 11\%$: the slopes obtained from a linear fit of
344 estimated and measured N_{CCN} in Fig 6 decreased rapidly (almost with a decrease of
345 ~50%) when the x_{org} varied from <40% to >60% at supersaturations of 0.075%, while
346 it didn't exhibit a lot of reduction (merely ~10%) along with the increasing of x_{org} for
347 the supersaturation of 0.76%. N_{CCN} was estimated most accurately at higher
348 supersaturation levels. This is likely because a large fraction of particles was already
349 CCN-active. Also, particle composition has relatively less influence on CCN
350 activation at high supersaturations (Twohy and Anderson, 2008). For the oxidized or
351 aged particles with $f_{44} > 15\%$, the slopes still follow the similar tendency with the
352 variations of x_{org} at low and high supersaturations but changed more smoothly to the
353 x_{org} attributing to the oxidized/aged organic particles being more hygroscopic.

354 However, the impacts of the aerosol particles oxidization level on estimating
355 N_{CCN} were also very significant. For example, when the particles were composed by

356 large amounts of organics ($x_{\text{org}} > 60\%$), the N_{CCN} at the supersaturation of 0.075% and
357 0.13% was underestimated by 46% and 44% respectively at $f_{44} < 11\%$, while the
358 underestimation decreased to 32% and 23% at the corresponding supersaturation level
359 at $f_{44} > 15\%$. The N_{CCN} at $ss = 0.76$ was underestimated by 11% and 4% respectively at
360 $f_{44} < 11\%$ and $f_{44} > 15\%$. One thus could conclude that the estimation of N_{CCN} would be
361 largely improved if the aerosol particles were aged with high oxidation level,
362 especially when the chemical composition of the particles is dominated by organics.
363 But for the particles with relative low organics ($x_{\text{org}} < 40\%$), the effect caused by the f_{44}
364 was quite insignificant both for high and low supersaturations. In Fig 6, the slopes
365 were all around 1.0 at the two cases of $f_{44} < 11\%$ and $f_{44} > 15\%$. This can be easily
366 explained. When x_{org} is less than 40%, the overall hygroscopicity of the particles is
367 dominated by inorganic species such as sulfate and nitrate, which are more
368 hygroscopic (κ_{inorg} usually larger than 0.6) than organic compounds (κ_{org}
369 usually smaller than 0.2). As a result, a larger fraction of particles can be
370 activated. According to the simple mixing rule based on chemical volume fractions
371 proposed by Petters and Kreidenweis (2007), the contribution from organics is quite
372 small. If x_{org} is greater than 60%, organics will dominate the overall particle
373 hygroscopicity. Particles with a large f_{44} are much more hygroscopic and thus strongly
374 influence the estimated N_{CCN} . Our results indicated that increasing the proportion of
375 secondary organics would decrease the uncertainties in estimating N_{CCN} and lead to a
376 more accurate estimation of N_{CCN} .

377 4.5 Applicability of CCN efficiency spectra

378 As a means of testing the applicability of the CCN activation spectra, campaign
379 mean CCN efficiency spectra at different supersaturations observed at the Xinzhou

380 site is used to estimate N_{CCN} at the Xinzhou and Xianghe sites respectively, which
381 helps to further examine the sensitivity of N_{CCN} to aerosol type. Data from the two
382 sites were measured during the warm season so that the effect of temporal variations
383 in aerosols on CCN levels is reduced. Fitted campaign mean CCN efficiency spectrum
384 at the five supersaturations at Xinzhou (corresponding to spectra in Fig. 1) is
385 multiplied by dry PSDs actually measured at Xinzhou and at the Xianghe site
386 respectively. This generates estimated CCN size distributions at the two sites. They
387 are then integrated over the whole size range (14-600 nm and 10-700 nm at the
388 Xinzhou and Xianghe sites, respectively) to obtain the estimated N_{CCN} . The measured
389 CCN size distributions at each site are integrated to produce the observed N_{CCN} .

390 Figure 7 shows estimated N_{CCN} as a function of measured N_{CCN} for different
391 supersaturation levels at the two sites. N_{CCN} at Xinzhou was underestimated by 4-5%
392 at supersaturation levels of 0.39% and 0.76%, and was slightly overestimated (~2%)
393 at Xianghe for the same supersaturation levels. Good agreement is seen at the 0.39%
394 and 0.76% supersaturation levels for data from both sites ($R^2 > 0.92$). N_{CCN} at
395 Xinzhou was underestimated by ~7% at supersaturation levels $< 0.1\%$ ($R^2 = 0.87$). At
396 Xianghe, however, N_{CCN} was overestimated by 19-23% at supersaturation levels $< 0.1\%$
397 although the correlation between calculated and measured N_{CCN} was good. Because
398 size-resolved CCN efficiency spectra were applied here, excluding the impact of
399 particle size, the influence of chemical composition on CCN activation can be
400 investigated. The poor estimates of CCN at low supersaturation levels could be
401 attributed to the high sensitivity of N_{CCN} to chemical composition. Because the mass
402 fractions of inorganics and organics measured at the two sites are similar (Fig. 1) and
403 the hygroscopicity for inorganic components is fixed, this overestimation is attributed
404 to the smaller proportion of aged and oxidized organic aerosols at Xianghe compared

405 with aerosols at Xinzhou ($f_{44} = 17\%$ and 11% at Xinzhou and Xianghe, respectively).

406 5. Summary and conclusions

407 In this study, we have investigated the impacts of particle physicochemical
408 properties on CCN activity based on field measurements obtained from 22 July to 26
409 August of 2014 in the suburb of Xinzhou, China. Five-day back trajectories combined
410 with measurements were analyzed to examine air mass influences on CCN activity.
411 CCN efficiency was largely reduced by local ~~primary biomass burning events~~
412 air masses, and the MAF was low to $<60\%$, suggesting externally-mixed and the
413 heterogeneity of particle composition for local emitted aerosols. The CCN activation
414 efficiency was enhanced significantly when the site was under the influence of air
415 transported from far away, during which aerosols could be mixed well with more
416 hygroscopic secondary organic and inorganic components. The relationship between
417 N_{CN} and N_{CCN} was generally poor. Large errors would arise if using the former to
418 estimate the latter, especially under low supersaturation conditions.

419 The sensitivity of N_{CCN} estimation to both x_{org} as well as f_{44} on estimating
420 N_{CCN} has also been examined. A strong dependence of N_{CCN} on the both two
421 parameters was noted. The sensitivity of N_{CCN} to volume fraction and particles
422 oxidization or aging level of organics to N_{CCN} increased with increasing increase of x_{org} .
423 And also this dependence weakens as the supersaturation level increases. When the
424 particles were mostly composed of organics ($x_{org} > 60\%$), the N_{CCN} at the
425 supersaturation of 0.075% and 0.13% was underestimated by 46% and 44%
426 respectively if aerosol particles were freshly emitted with primary organics ($f_{44} < 11\%$);
427 while the underestimation decreased to 32% and 23% at the corresponding
428 supersaturations if the particles were with more hygroscopic secondary
429 organics ($f_{44} > 15\%$). The N_{CCN} at the supersaturation of 0.76% was underestimated by

带格式的

430 11% and 4% respectively at $f_{44} < 11\%$ and $f_{44} > 15\%$. But for the particles composed of
431 low organics (e.g. $x_{\text{org}} < 40\%$), the effect caused by the f_{44} was quite insignificant both
432 at high and low supersaturations. This is due to that the overall hygroscopicity of the
433 particles is dominated by inorganics such as sulfate and nitrate, which are more
434 hygroscopic than organic compounds. Our results indicated that it would ~~decrease the~~
435 ~~uncertainties in estimating N_{CCN} and~~ lead to a more accurate estimation of N_{CCN} to
436 increase the proportion of secondary organics, especially when the composition of the
437 aerosols is dominated by organics.

带格式的: 字体: Times New Roman

438 The applicability of the CCN efficiency spectrum measured at the Xinzhou site
439 to the Xianghe site was examined and a good agreement was found when the
440 supersaturation level was $> 0.2\%$. However, N_{CCN} at the Xianghe site was
441 overestimated by 19-23% when the supersaturation level was $< 0.1\%$. Because of the
442 similar mass fractions of inorganics and organics measured at the two sites, we
443 conclude that this overestimation was mainly caused by the smaller proportion of
444 aged and oxidized organic aerosols at Xianghe compared with aerosols at Xinzhou.

445 **Acknowledgements**

446 This work was funded by the National Basic Research Program of China '973' (Grant
447 No. 2013CB955801, 2013CB955804), the Fundamental Research Funds for the
448 Central Universities (Grant No. 2013YB35) and the NSCF-TAMU Collaborative
449 Research Grant Program (Grant No. 4141101031). We also acknowledge the members
450 of the A²C² team for their hard work during the campaign, including Mr. Du Wei
451 (from the State Key Laboratory of Atmospheric Boundary Layer Physics and
452 Atmospheric Chemistry of the Institute of Atmospheric Physics/Chinese Academy of
453 Sciences for carrying out the chemical composition measurements) and Mr. Yuan
454 Cheng (from Nanjing University who helped make the size-resolved CCNc

455 measurements).

456 **References**

- 457 Aiken, A. C., DeCarlo, P. F., Kroll, J. H., Worsnop, D. R., Huffman, J. A., Docherty,
458 K. S., Ulbrich, I. M., Mohr, C., Kimmel, J. R., Sueper, D., Sun, Y., Zhang, Q.,
459 Trimborn, A., Northway, M., Ziemann, P. J., Canagaratna, M. R., Onasch, T. B.,
460 Alfarra, M. R., Prevot, A. S. H., Dommen, J., Duplissy, J., Metzger, A.,
461 Baltensperger, U., and Jimenez, J. L.: O/C and OM/OC ratios of primary,
462 secondary, and ambient organic aerosols with high-resolution time-of-flight aerosol
463 mass spectrometry, *Environ. Sci. Technol.*, 42, 4478–4485, 2008.
- 464 Andreae, M.O.: Correlation between cloud condensation nuclei concentration and
465 aerosol optical thickness in remote and polluted regions, *Atmos. Chem. Phys.*, 9,
466 543-556, 2009.
- 467 Bougiatioti, A., Fountoukis, C., Kalivitis, N., Pandis, S. N., Nenes, A., and
468 Mihalopoulos, N.: Cloud condensation nuclei measurements in the marine
469 boundary layer of the eastern Mediterranean: CCN closure and droplet growth
470 kinetics. *Atmos. Chem. Phys.*, 9, 7053–7066, 2009.
- 471 Bougiatioti, A., Nenes, A., Fountoukis, C., Kalivitis, N., Pandis, S. N., and
472 Mihalopoulos, N.: Size-resolved CCN distributions and activation kinetics of aged
473 continental and marine aerosol, *Atmos. Chem. Phys.*, 11, 8791-8808,
474 doi:10.5194/acp-11-8791-2011, 2011.
- 475 Chuang, P. Y., Collins, D. R., Pawlowska, H., Snider, J. R., Jonsson, H. H., Brenguier,
476 J. L., Flagan, R. C., and Seinfeld, J. H.: CCN measurements during ACE-2 and
477 their relationship to cloud microphysical properties, *Tellus B*, 52, 843–867, 2000.
- 478 Clarke, A., McNaughton, C., Kasputin, V. N., Shinozuka, Y., Howell, S., Dibb, J.,
479 Zhou, J., Anderson, B., Brekhovskikh, V., Turner, H., and Pinkerton, M.: Biomass

- 480 burning and pollution aerosol over North America: Organic components and their
481 influence on spectral optical properties and humidification response, *J. Geophys.*
482 *Res.*, 112, D12S18, doi:10.1029/2006JD007777, 2007.
- 483 Dal Maso, M., L. Sogacheva, P. P. Aalto, I. Riipinen, M. Komppula, P. Tunved, L.
484 Korhonen, V. SUURUSKI, A. Hirsikko, and T. KurtEN, Aerosol size
485 distribution measurements at four Nordic field stations: identification, analysis
486 and trajectory analysis of new particle formation bursts, *Tellus B*, 2007, 59(3),
487 350-361.
- 488 Deng, Z., Zhao, C., Ma, N., Liu, F., Ran, L., Xu, W., Liang, Z., Liang, S., Huang, M.,
489 Ma, X., Zhang, Q., Quan, J., and Yan, P.: Size- resolved and bulk activation
490 properties of aerosols in the North China Plain. *Atmos. Chem. Phys.*, 11,
491 3835-3846, 2011.
- 492 Deng, Z., Zhao, C., Ma, N., Ran, L., Zhou, G., Lu, D., and Zhou, X.: An examination
493 of parameterizations for the CCN number concentration based on in situ
494 measurements of aerosol activation properties in the North China Plain, *Atmos.*
495 *Chem. Phys.*, 13, 6227–6237, doi:10.5194/acp-13-6227-2013, 2013.
- 496 Draxler, R., R. and Hess, G., D. 1998. An overview of the HYSPLIT 4 modeling
497 system for trajectories, dispersion, and deposition, *Aust. Meteorol. Mag.* 47, 295–
498 308.
- 499 Duplissy, J., DeCarlo, P. F., Dommen, J., Alfarra, M. R., Metzger, A., Barmpadimos,
500 I., Prevot, A. S. H., Weingartner, E., Tritscher, T., Gysel, M., Aiken, A. C., Jimenez,
501 J. L., Canagaratna, M. R., Worsnop, D. R., Collins, D. R., Tomlinson, J., and
502 Baltensperger, U.: Relating hygroscopicity and composition of organic aerosol
503 particulate matter, *Atmos. Chem. Phys.*, 11, 1155–1165,
504 doi:10.5194/acp-11-1155-2011, 2011.

- 505 Dusek, U., Covert, D. S., Wiedensohler, A., Neususs, C., Weise, D., and Cantrell, W.:
506 Cloud condensation nuclei spectra derived from size distributions and hygroscopic
507 properties of the aerosol in coastal south-west Portugal during ACE-2, *Tellus B*, 55,
508 35–53, 2003.
- 509 Engelhart, G. J., Hennigan, C. J., Miracolo, M. A., Robinson, A. L., and Pandis, S. N.:
510 Cloud condensation nuclei activity of fresh primary and aged biomass burning
511 aerosol, *Atmos. Chem. Phys.*, 12, 7285–7293, doi:10.5194/acp-12-7285-2012,
512 2012.
- 513 Ervens, B., Cubison, M. J., Andrews, E., Feingold, G., Ogren, J.A., Jimenez, J. L.,
514 Quinn, P. K., Bates, T. S., Wang, J., Zhang, Q., Coe, H., Flynn, M., and Allan, J. D.:
515 CCN predictions using simplified assumptions of organic aerosol composition and
516 mixing state: a synthesis from six different locations, *Atmos. Chem. Phys.*, 10,
517 4795–4807, doi:10.5194/acp-10-4795-2010, 2010.
- 518 Gasparini, R., Collins, D. R., Andrews, E., Sheridan, P. J., Ogren, J. A., and Hudson, J.
519 G.: Coupling aerosol size distributions and size-resolved hygroscopicity to predict
520 humidity-dependent optical properties and cloud condensation nuclei spectra., *J.*
521 *Geophys. Res.*, 111, D05S13, doi:10.1029/2005JD006092, 2006.
- 522 Gunthe SS; Rose D; Su H; Garland RM; Achtert P; Nowak A; Wiedensohler A;
523 Kuwata M; Takegawa N; Kondo Y; Hu M; Shao M; Zhu T; Andreae MO; Pöschl
524 U (2011) Cloud condensation nuclei (CCN) from fresh and aged air pollution in
525 the megacity region of Beijing, *Atmospheric Chemistry and Physics*, 11,
526 pp.11023-11039. doi: 10.5194/acp-11-11023-2011
- 527 Guo, S., Hu, M., Zamora, M. L., Peng, J., Shang, D., Zheng, J., Zhuofei Du, Zhijun
528 Wu, Min Shao, Limin Zeng, Mario J. Molina,¹ and Zhang, R. (2014).
529 Elucidating severe urban haze formation in China. *Proceedings of the National*

- 530 Academy of Sciences of the United States of America, 111(49), 17373–17378.
531 doi:10.1073/pnas.1419604111
- 532 Hartz, K. E. H., Tischuk, J. E., Chan, M. N., Chan, C. K., Donahue, N. M., and Pandis,
533 S. N.: Cloud condensation nuclei activation of limited solubility organic aerosol,
534 *Atmos. Environ.*, 40, 605–617, 2006.
- 535 Hings, S. S., Wrobel, W. C., Cross, E. S., Worsnop, D. R., Davidovits, P., and Onasch,
536 T. B.: CCN activation experiments with adipic acid: effect of particle phase and
537 adipic acid coatings on soluble and insoluble particles, *Atmos. Chem. Phys.*, 8,
538 3735–3748, doi:10.5194/acp-8-3735-2008, 2008.
- 539 Hudson, J. G. and Da, X. Y.: Volatility and size of cloud condensation nuclei, *J.*
540 *Geophys. Res.*, 101, 4435–4442, 1996.
- 541 Hussein, T., M. Dal Maso, T. PETÄJÄ, I. K. KOPONEN, P. PAATERO, P. P.
542 AALTO, K. HÄMERI, and M. KULMALA, Evaluation of an automatic
543 algorithm for fitting the particle number size distributions, *BOREAL*
544 *ENVIRONMENT RESEARCH*, 2005, 10(5), 337-355.
- 545 Junge, C. and McLaren, E.: Relationship of cloud nuclei spectra to aerosol size
546 distribution and composition, *J. Atmos. Sci.*, 28, 382–390, 1971.
- 547 Kammermann, L., Gysel, M., Weingartner, E., Herich, H., Cziczo, D. J., Holst, T.,
548 Svenningsson, B., Arneth, A., and Baltensperger, U.: Subarctic atmospheric aerosol
549 composition: 3. Measured and modeled properties of cloud condensation nuclei, *J.*
550 *Geophys. Res.*, 115, D04202, doi:10.1029/2009JD012447, 2010.
- 551 Köhler, H.: The nucleus in and growth of hygroscopic droplets, *Trans. Faraday Soc.*,
552 32, 1152–1161, doi:10.1039/TF9363201152, 1936.
- 553 Lance, S., Medina, J., Smith, J., and Nenes, A.: Mapping the operation of the DMT
554 continuous flow CCN counter, *Aerosol Sci. Technol.*, 40, 242–254, 2006.

- 555 Latham, T. L., Beyersdorf, A. J., Thornhill, K. L., Winstead, E. L., Cubison, M. J.,
556 Hecobian, A., Jimenez, J. L., Weber, R. J., Anderson, B. E., and Nenes, A.: Analysis
557 of CCN activity of Arctic aerosol and Canadian biomass burning during summer
558 2008, *Atmos. Chem. Phys.*, 13, 2735-2756, doi:10.5194/acp-13-2735-2013, 2013.
- 559 Lee, Y. S., Collins, D. R., Li, R. J., Bowman, K. P., and Feingold, G.: Expected
560 impact of an aged biomass burning aerosol on cloud condensation nuclei and cloud
561 droplet concentrations, *J. Geophys. Res.*, 111, D22204, doi:10.1029/2005JD006464,
562 2006.
- 563 Li, Z., Chen, H., Cribb, M., Dickerson, R. E., Holben, B., Li, C., Lu, D., Luo, Y.,
564 Maring, H., Shi, G., Tsay, S.-C., Wang, P., Wang, Y., Xia, X., Zheng, Y., Yuan, T.,
565 and Zhao, F.: Preface to special section on East Asian Studies of Tropospheric
566 Aerosols: An International Regional Experiment (EASTAIRE), *J. Geophys. Res.*,
567 112, D22S00, doi:10.1029/2007JD008853, 2007.
- 568 Li, Z., Li, C., Chen, H., Tsay, S.-C., Holben, B., Huang, J., Li, B., Maring, H., Qian,
569 Y., Shi, G., Xia, X., Yin, Y., Zheng, Y., and Zhuang, G.: East Asian Studies of
570 Tropospheric Aerosols and Impact on Regional Climate (EAST - AIRC): An
571 overview, *J. Geophys. Res.*, 116, D00K34, doi:10.1029/2010JD015257, 2011.
- 572 Liu, X. and Wang, J.: How important is organic aerosol hygroscopicity to aerosol
573 indirect forcing? *Environ. Res. Lett.*, 5, 044010,
574 doi:10.1088/1748-9326/5/4/044010, 2010.
- 575 McFiggans, G., Artaxo, P., Baltensperger, U., Coe, H., Facchini, M. C., Feingold, G.,
576 Fuzzi, S., Gysel, M., Laaksonen, A., Lohmann, U., Mentel, T. F., Murphy, D. M.,
577 O'Dowd, C. D., Snider, J. R., and Weingartner, E.: The effect of physical and
578 chemical aerosol properties on warm cloud droplet activation, *Atmos. Chem. Phys.*,
579 6, 2593–2649, doi:10.5194/acp-6-2593-2006, 2006.

- 580 Mei, F., Hayes, P. L., Ortega, A. M., Taylor, J. W., Allan, J. D., Gilman, J. B., Kuster,
581 W. C., de Gouw, J. A., Jimenez, J. L., and Wang, J.: Droplet activation properties
582 of organic aerosols observed at an urban site during CalNex-LA, *J. Geophys. Res.*,
583 118(7), 2903-2917, doi: 10.1002/jgrd.50285, 2013b.
- 584 Mei, F., Setyan, A., Zhang, Q., and Wang, J.: CCN activity of organic aerosols
585 observed downwind of urban emissions during CARES, *Atmos. Chem. Phys.*, 13,
586 12155–12169, doi:10.5194/acp-13-12155-2013, 2013a.
- 587 ~~Mikhailov, E., Vlasenko, S., Martin, S. T., Koop, T., and Pöschl, U.: Amorphous
588 and crystalline aerosol particles interacting with water vapor: conceptual
589 framework and experimental evidence for restructuring, phase transitions and
590 kinetic limitations, *Atmos. Chem. Phys.*, 9, 9491–9522,
591 doi:10.5194/acp-9-9491-2009, 2009.~~
- 592 Mircea, M., Facchini, M. C., Decesari, S., Cavalli, F., Emblico, L., Fuzzi, S., Vestin,
593 A., Rissler, J., Swietlicki, E., Frank, G., Andreae, M. O., Maenhaut, W., Rudich, Y.,
594 and Artaxo, P.: Importance of the organic aerosol fraction for modeling aerosol
595 hygroscopic growth and activation: a case study in the Amazon Basin, *Atmos.*
596 *Chem. Phys.*, 5, 3111–3126, 2005, <http://www.atmos-chem-phys.net/5/3111/2005/>.
- 597 Ng, N. L., Herndon, S. C., Trimborn, A., Canagaratna, M. R., Croteau, P. L., Onasch,
598 T. B., Sueper, D., Worsnop, D. R., Zhang, Q., Sun, Y. L., and Jayne, J. T.: An
599 Aerosol Chemical Speciation Monitor (ACSM) for Routine Monitoring of the
600 Composition and Mass Concentrations of Ambient Aerosol, *Aerosol Sci. Tech.*, 45,
601 770–784, 2011.
- 602 Paramonov, M., Aalto, P. P., Asmi, A., Prisle, N., Kerminen, V.-M., Kulmala, M., and
603 Petäjä T.: The analysis of size-segregated cloud condensation nuclei counter
604 (CCNC) data and its implications for aerosol-cloud interactions, *Atmos. Chem.*

- 605 Phys. Discuss., 13, 9681-9731, doi:10.5194/acpd-13-9681-2013, 2013.
- 606 Petters, M. D., and Kreidenweis, S. M.: A single parameter representation of
607 hygroscopic growth and cloud condensation nucleus activity, *Atmos. Chem. Phys.*,
608 7, 1961–1971, doi:10.5194/acp-7-1961-2007, 2007.
- 609 Petters, M. D. and Kreidenweis, S. M.: A single parameter representation of
610 hygroscopic growth and cloud condensation nucleus activity – Part 2: Including
611 solubility, *Atmos. Chem. Phys.*, 8, 6273–6279, doi:10.5194/acp-8-6273-2008,
612 2008.
- 613 Raymond, T. M., and Pandis, S. N.: Cloud activation of single component organic
614 aerosol particles, *J. Geophys. Res.*, 107, 4787, doi:10.1029/2002JD002159, 2002.
- 615 Reutter, P., Su, H., Trentmann, J., Simmel, M., Rose, D., Gunthe, S. S., Wernli, H.,
616 Andreae, M. O., and Pöschl, U.: Aerosol- and updraft-limited regimes of cloud
617 droplet formation: influence of particle number, size and hygroscopicity on the
618 activation of cloud condensation nuclei (CCN), *Atmos. Chem. Phys.*, 9, 7067–7080,
619 doi:10.5194/acp-9-7067-2009, 2009.
- 620 Rissler, J., Swietlicki, E., Zhou, J., Roberts, G., Andreae, M. O., Gatti, L. V., and
621 Artaxo, P.: Physical properties of the submicrometer aerosol over the Amazon rain
622 forest during the wet to dry season transition – comparison of modeled and
623 measured CCN concentrations, *Atmos. Chem. Phys.*, 4, 2119–2143,
624 <http://www.atmos-chem-phys.net/4/2119/2004/>, 2004.
- 625 Rissler, J., Vestin, A., Swietlicki, E., Fisch, G., Zhou, J., Artaxo, P., and Andreae, M.
626 O.: Size distribution and hygroscopic properties of aerosol particles from
627 dry-season biomass burning in Amazonia, *Atmos. Chem. Phys.*, 6, 471–491,
628 doi:10.5194/acp-6-471-2006, 2006.
- 629 Rose, D., Gunthe, S. S., Mikhailov, E., Frank, G. P., Dusek, U., Andreae, M. O., and

- 630 Poschl, U.: Calibration and measurement uncertainties of a continuous-flow cloud
631 condensation nuclei counter (DMT-CCNC): CCN activation of ammonium sulfate
632 and sodium chloride aerosol particles in theory and experiment, *Atmos. Chem.*
633 *Phys.*, 8, 1153–1179, 2008, <http://www.atmos-chem-phys.net/8/1153/2008/>.
- 634 Rose, D., Nowak, A., Achtert, P., Wiedensohler, A., Hu, M., Shao, M., Zhang, Y.,
635 Andreae, M. O., and Poschl, U.: Cloud condensation nuclei in polluted air and
636 biomass burning smoke near the mega-city Guangzhou, China – Part 1:
637 Size-resolved measurements and implications for the modeling of aerosol particle
638 hygroscopicity and CCN activity, *Atmos. Chem. Phys.*, 10, 3365–3383,
639 doi:10.5194/acp-10-3365-2010, 2010.
- 640 Rousseau, D., D., Duzer, D., Etienne, J., L., Cambon, G., Jolly, D. And coauthors.
641 2004. Pollen record of rapidly changing air trajectories to the North Pole, *J.*
642 *Geophys. Res.* 109, D06116, doi:10.1029/2003JD003985.
- 643 Snider, J.R., Guibert, S., Brenguierand, J. L. and Putaud, J. P.: Aerosol activation in
644 marine stratocumulus clouds: Part – II Köhler and parcel theory closure studies, *J.*
645 *Geophys. Res.*, 108, doi:10.1029/2002JD002692, 2003
- 646 Sotiropoulou, R. E. P., Nenes, A., Adams, P. J., and Seinfeld, J. H.: Cloud
647 condensation nuclei prediction error from application of Köhler theory:
648 Importance for the aerosol indirect effect, *J. Geophys. Res.*, 112, D12202,
649 doi:10.1029/2006JD007834, 2007.
- 650 Stohl, A. 1996, Trajectory statistics - a new method to establish source-receptor
651 relationships of air pollutants and its application to the transport of particulate
652 sulfate in Europe, *Atmos. Environ.* 30, 579–587.
- 653 Stroud, C. A., Nenes, A., Jimenez, J. L., DeCarlo, P., Huffman, J. A., Brientjes, R.,
654 Nemitz, E., Delia, A. E., Toohey, D. W., Guenther, A. B., and Nandi, S.: Cloud

- 655 Activating Properties of Aerosol Observed during CELTIC, *J. Atmos. Sci.*, **64**, 441–
656 459, 2007.
- 657 Sun, Y., Wang, Z., Dong, H., Yang, T., Li, J., Pan, X., Chen, P., and Jayne, J. T.:
658 Characterization of summer organic and inorganic aerosols in Beijing, China with
659 an Aerosol Chemical Speciation Monitor, *Atmos. Environ.*, **51**, 250–259,
660 doi:10.1016/j.atmosenv.2012.01.013, 2012.
- 661 Takegawa, N., Miyakawa, T., Kawamura, K., and Kondo, Y.: Contribution of selected
662 di-carboxylic and omega-oxocarboxylic acids in ambient aerosol to the m/z 44
663 signal of an aerodyne aerosol mass spectrometer, *Aerosol Sci. Technol.*, **41**, 418–
664 437, doi:10.1080/02786820701203215, 2007.
- 665 Twohy, C. H. and Anderson, J. R.: Droplet nuclei in non-precipitating clouds:
666 composition and size matter, *Environ. Res. Lett.*, **3**, 045002,
667 doi:10.1088/1748-9326/3/4/045002, 2008.
- 668 VanReken, T. M., Rissman, T. A., Roberts, G. C., Varutbangkul, V., Jonsson, H. H.,
669 Flagan, R. C., and Seinfeld, J. H.: Toward aerosol/cloud condensation nuclei (CCN)
670 closure during CRYSTAL-FACE, *J. Geophys. Res.*, **108**, 4633,
671 doi:10.1029/2003JD003582, 2003.
- 672 VanReken, T. M., Ng, N. L., Flagan, R. C., and Seinfeld, J. H.: Cloud condensation
673 nucleus activation properties of biogenic secondary organic aerosol, *J. Geophys.*
674 *Res.*, **110**, D07206, doi:10.1029/2004JD005465, 2005.
- 675 Varutbangkul, V., Brechtel, F. J., Bahreini, R., Ng, N. L., Keywood, M. D., Kroll, J.
676 H., Flagan, R. C., Seinfeld, J. H., Lee, A., and Goldstein, A. H.: Hygroscopicity of
677 secondary organic aerosols formed by oxidation of cycloalkenes, monoterpenes,
678 sesquiterpenes, and related compounds, *Atmos. Chem. Phys.*, **6**, 2367–2388, 2006.
- 679 Verver, G., F. Raes, D. Vogelesang, and D. Johnson, The 2nd Aerosol characterization

- 680 Experiment (ACE-2): meteorological and chemical context, *Tellus B*, 2000,52(2),
681 126-140.
- 682 Wang, J., Lee, Y.-N., Daum, P. H., Jayne, J., and Alexander, M. L.: Effects of aerosol
683 organics on cloud condensation nucleus (CCN) concentration and first indirect
684 aerosol effect, *Atmos. Chem. Phys.*, 8, 6325–6339, doi:10.5194/acp-8-6325-2008,
685 2008.
- 686 Wang, Y.Q., Zhang, X.Y. and Draxler, R., 2009. TrajStat: GIS-based software that
687 uses various trajectory statistical analysis methods to identify potential sources
688 from long-term air pollution measurement data. *Environmental Modelling &*
689 *Software*, 24: 938-939
- 690 Ward, D. S., Eidhammer, T., Cotton, W. R., and Kreidenweis, S. M.: The role of the
691 particle size distribution in assessing aerosol composition effects on simulated
692 droplet activation, *Atmos. Chem. Phys.*, 10, 5435–5447,
693 doi:10.5194/acp-10-5435-2010, 2010.
- 694 Weber, R., P. H. McMurry, R. Mauldin, D. Tanner, F. Eisele, A. Clarke, and V.
695 Kapustin, New particle formation in the remote troposphere: A comparison of
696 observations at various sites, *Geophysical Research Letters*, 1999,26(3),
697 307-310.
- 698 Wex, H., Hennig, T., Salma, I., Ocskay, R., Kiselev, A., Henning, S., Massling, A.,
699 Wiedensohler, A., and Stratmann, F.: Hygroscopic growth and measured and
700 modeled critical super-saturations of an atmospheric HULIS sample, *Geophys. Res.*
701 *Lett.*, 34, L02818, doi:10.1029/2006GL028260, 2007.
- 702 Whitby, K., T.: The physical characteristics of sulfur aerosols. *Atmos. Environ.*, 12,
703 135-159, 1967, Online publication date: 1-Jan-1978, 1978.
- 704 Wiedensohler A; Cheng YF; Nowak A; Wehner B; Achtelt P; Berghof M; Birmili W;

705 Wu ZJ; Hu M; Zhu T; Takegawa N; Kita K; Kondo Y; Lou SR; Hofeumahaas A;
706 Holland F; Wahner A; Gunthe SS; Rose D; Su H; Pöschl U (2009) Rapid aerosol
707 particle growth and increase of cloud condensation nucleus activity by secondary
708 aerosol formation and condensation: A case study for regional air pollution in
709 northeastern China, *Journal of Geophysical Research: Atmospheres*, 114, . doi:
710 [10.1029/2008JD010884](https://doi.org/10.1029/2008JD010884)

711 Yue, D. L., Hu, M., Zhang, R. J., Wu, Z. J., Su, H., Wang, Z. B., Peng, J. F., He, L.Y.,
712 Huang, X. F., Gong, Y. G., and Wiedensohler, A.: Potential contribution of new
713 particle formation to cloud condensation nuclei in Beijing, *Atmos. Environ.*, 45,
714 6070-6077, 2011.

715 Zhang, Q., Meng, J., Quan, J., Gao, Y., Zhao, D., Chen, P., and He, H.: Impact of
716 aerosol composition on cloud condensation nuclei activity, *Atmos. Chem. Phys.*, 12,
717 3783-3790, doi:10.5194/acp-12-3783-2012, 2012.

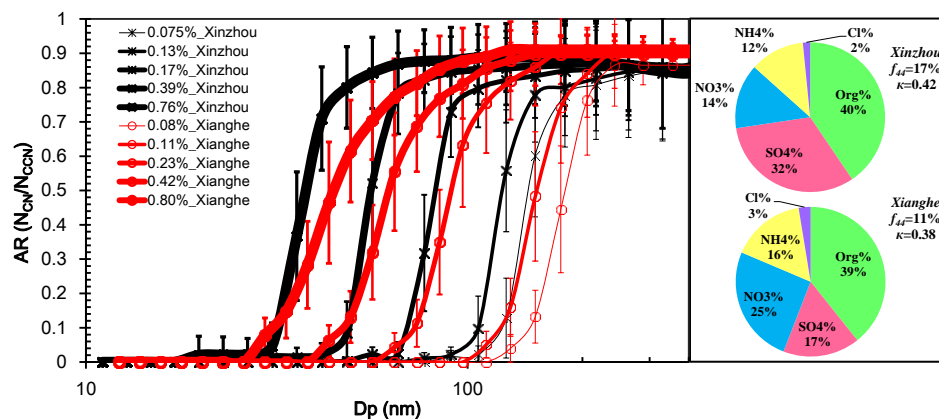
718 Zhang, F., Z. Li, R. J. Li, L. Sun, C. Zhao, P. C. Wang, Y. L. Sun, Y. N. Li, X. G. Liu,
719 J. X. Li, P. R. Li, G. Ren, and T. Y. Fan., Aerosol hygroscopicity and cloud
720 condensation nuclei activity during the AC3Exp campaign: implications for cloud
721 condensation nuclei parameterization. *Atmos. Chem. Phys.*, 14, 13423–13437,
722 2014

723
724
725
726
727
728
729
730
731

732 **Figures**

733

734



735

736 **Fig. 1.** Mean CCN efficiency spectra at the Xinzhou site (black lines with asterisks)
 737 measured from 22 July-26 August 2014 and at the Xianghe site (red lines with circles)
 738 site measured from 7-21 July 2013 for different supersaturation levels. Error bars
 739 representing one standard deviation are shown. Right panels show particle chemical
 740 composition in terms of mass concentration fractions at Xinzhou (top panel) and
 741 Xianghe (bottom panel) during their respective observation periods. The campaign
 742 average mass concentration of PM₁ is 31.6 $\mu\text{g m}^{-3}$ and 72.4 $\mu\text{g m}^{-3}$ at Xinzhou and
 743 Xianghe respectively. Note that the preset supersaturation levels were 0.07%, 0.1%,
 744 0.2%, 0.4% and 0.8% at both sites, but effective supersaturation levels showed
 745 slightly different after calibration.

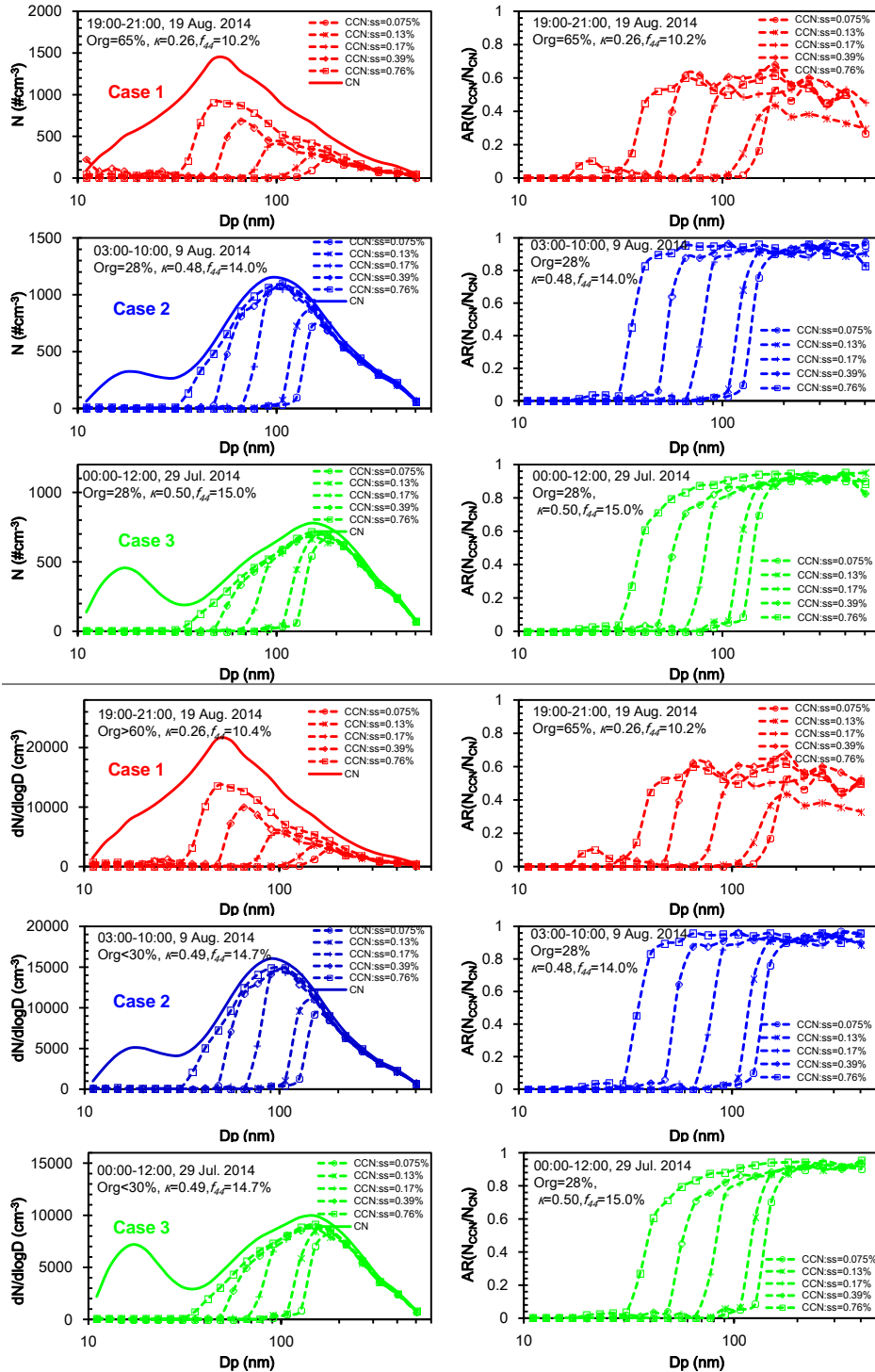
746

747

748

749

750



751

752

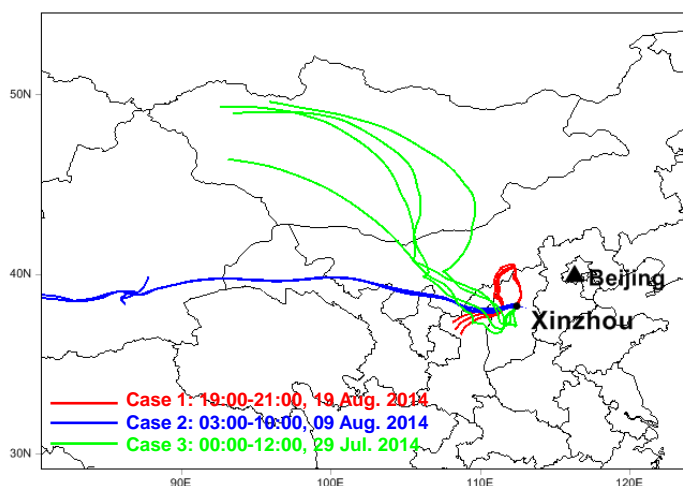
753

754

755

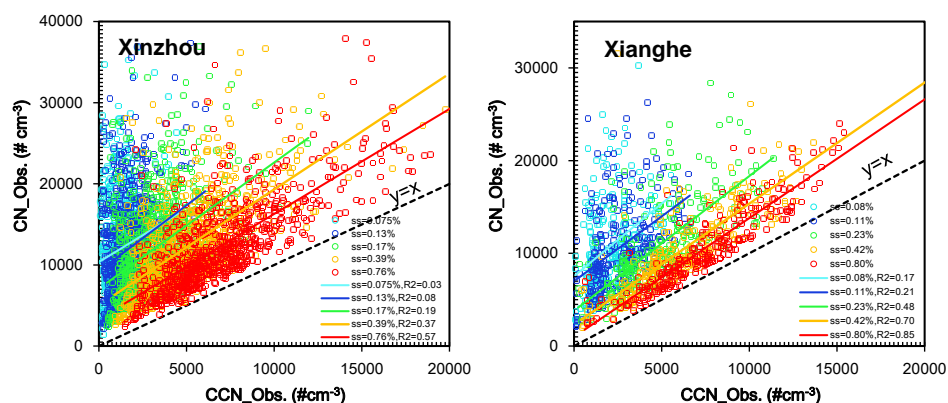
Fig. 2. Particle number size distribution (PSD) and CCN size distributions (left panels) and CCN efficiency spectra (right panels) at different supersaturation levels for Case 1 (upper panels, 19 August 2014, 19:00-21:00 LT), Case 2 (middle panels, 9 August

756 2014, 03:00-10:00 LT), and Case 3 (bottom panels, 29 July 2014, 00:00-12:00 LT).
 757 | Total CN number concentrations are 16671 cm⁻³, 12869 cm⁻³, and 10134 cm⁻³ for
 758 Case 1, Case 2, and Case 3, respectively. Mass concentrations of PM₁ are 28.36 μg
 759 m⁻³, 81.45 μg m⁻³, and 78.73 μg m⁻³ for Case 1, Case 2 and Case 3, respectively.
 760
 761
 762
 763
 764
 765
 766
 767
 768
 769



770
 771 **Fig. 3.** Five-day back trajectories for Case 1 (in red), Case 2 (in blue), and Case 3 (in
 772 green) calculated using the Hybrid Single-Particle Lagrangian Integrated Trajectory
 773 model with National Centers for Environmental Prediction reanalysis data. The arrival
 774 height of the trajectories at the Xinzhou site was at the surface.
 775
 776
 777
 778
 779

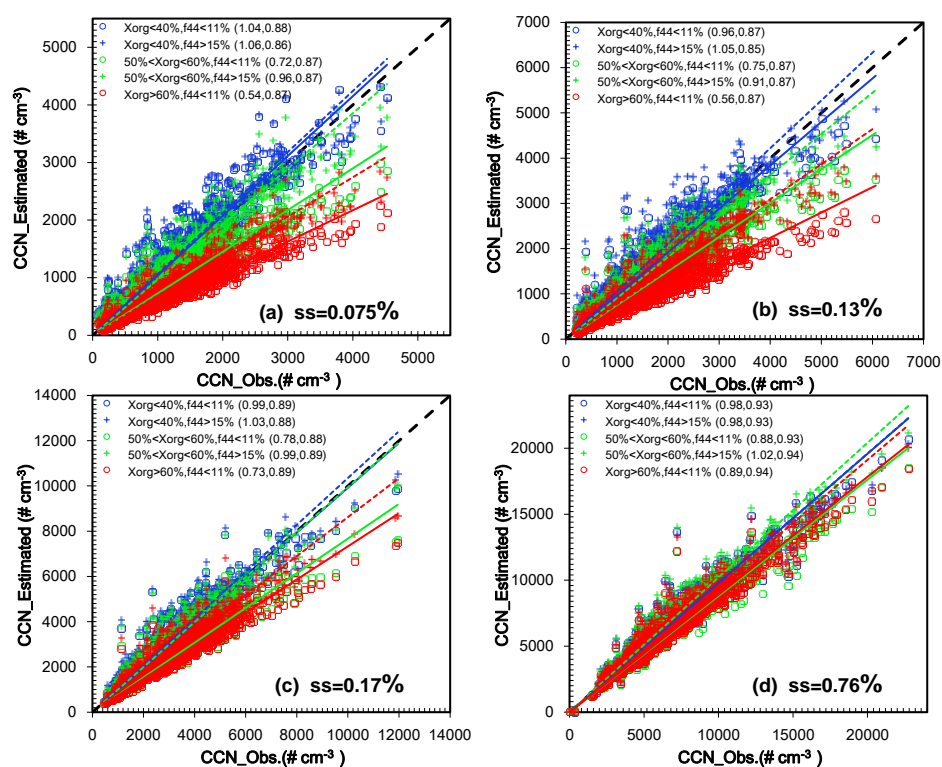
780
781
782
783
784
785
786
787
788
789
790
791
792
793



794
795
796
797
798
799
800
801
802
803
804
805
806

Fig. 4. Measured N_{CN} as a function of measured N_{CCN} for different supersaturation levels at the Xinzhou (left panel) and Xianghe (right panel) sites. The scatterplot between CCN_{Obs} and CN_{Obs} , were fitted with a linear function (in colored lines) and R^2 refer to the correlations of them.

807
808
809
810
811
812
813
814
815
816
817
818
819
820

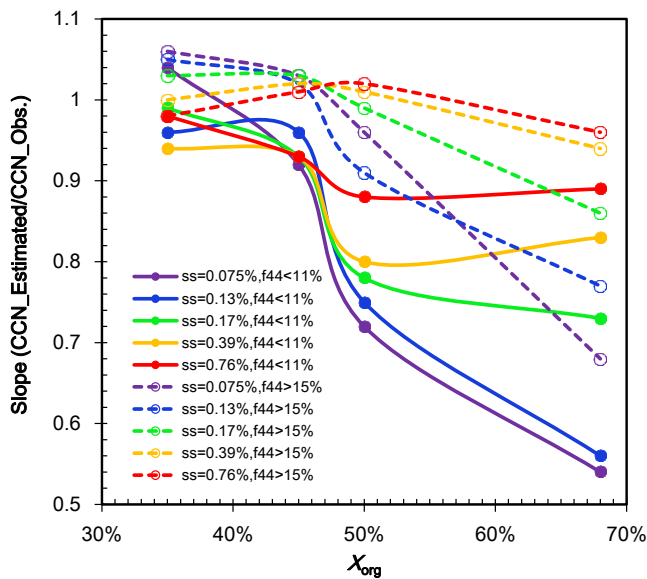


821
822
823
824

Fig. 5. The sensitivity of N_{CCN} to both organics volume fraction (x_{org}) as well as and oxidation level (using f_{44} , the fraction of m/z 44 in total organics, as an indicator aerosol organic material) of organics to estimation of N_{CCN} at supersaturation

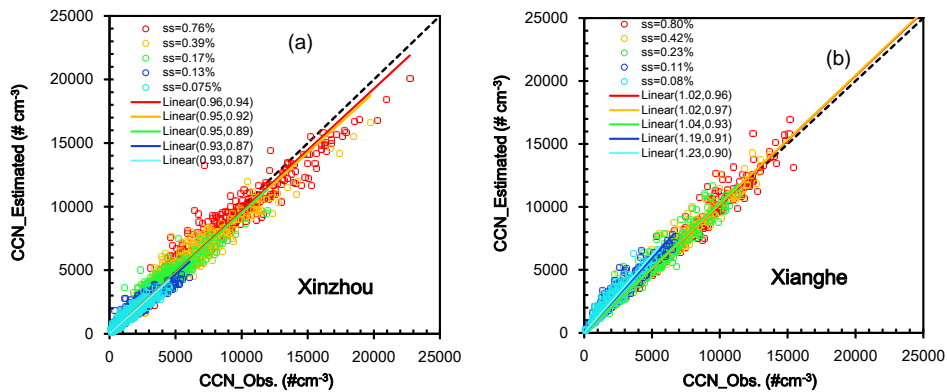
825 levels of (a) 0.075%, (b) 0.13%, (c) 0.17% and (d) 0.76% for cases when $x_{org} = 35\%$
 826 (blue circles), 52% (green circles), and 66% (red circles). The size-resolved CCN
 827 data were sorted when the $x_{org} > 60\%$, $50\% < x_{org} < 60\%$, $40\% < x_{org} < 50\%$ and $x_{org} < 40\%$
 828 respectively to do the sensitivity examination. The results of $40\% < x_{org} < 50\%$ was not
 829 plotted here. Mean values of the hygroscopic parameter κ_{chem} at $f_{44} < 11\%$ when
 830 $x_{org} > 60\%$, $50\% < x_{org} < 60\%$, $40\% < x_{org} < 50\%$ and $x_{org} < 40\%$ are 0.27, 0.34, 0.40 and
 831 0.46, respectively; while at $f_{44} > 15\%$ the value increased to 0.36, 0.42, 0.46 and 0.50
 832 respectively. Linear best-fit lines through each group of points are shown. Slopes and
 833 R^2 values are given in parentheses.

834
835
836
837
838
839
840
841
842
843
844
845



846

847 **Fig. 6.** Slopes of the linear fit of estimated and observed N_{CCN} dependence on volume
 848 fraction of organics (x_{org}) at $f_{44}<11\%$ and $f_{44}>15\%$ for different supersaturation levels.
 849 Mean values of the hygroscopic parameter κ_{chem} at $f_{44}<11\%$ when $x_{org}>60\%$, $50\%<x_{org}$
 850 $<60\%$, $40\%<x_{org}<50\%$ and $x_{org}<40\%$ are 0.27, 0.34, 0.40 and 0.46, respectively;
 851 while at $f_{44}>15\%$ the value increased to 0.36, 0.42, 0.46 and 0.50 respectively.



868
 869
 870 **Fig. 7.** Estimated N_{CCN} as a function of observed N_{CCN} for different supersaturation
 871 levels at (a) Xinzhou and (b) Xianghe. Note that the campaign mean CCN efficiency
 872 spectra at Xinzhou are used for estimating N_{CCN} at Xianghe. Linear best-fit lines

873 through each group of points are shown. Slopes and R^2 values are given in
874 parentheses.

875

876

877

878

879

880

881